A TIME-DEPENDENT FLAME MODEL UTILIZING THE METHOD OF LINES

H.D. Ladouceur and J.W. Fleming
Chemistry Division, Code 6110, Naval Research Laboratory
Washington, DC 20375-5000

Keywords: flame modeling, time-dependent model, method of lines

ABSTRACT

We have developed a time-dependent flame model to interpret the temporal evolution of various chemical species generated by laser photolysis of a steady-state low-pressure (10 torr) CH_4/O_2 flame. The model includes the effects of diffusion, convection and elementary chemical kinetics. The diffusion and convection terms are represented by finite difference expressions in the species conservation equations which reduce them to a stiff system of ordinary differential equations. The latter system is solved as an initial value problem by Gear's method. The initial conditions on the model are determined by a photolysis mechanism which perturbs concentrations of the steady-state flame. The computations demonstrate the importance in low-pressure flames of mass transport and chemistry in the relaxation of the perturbed state.

I. INTRODUCTION

This paper describes a time-dependent flame model which utilizes the method of lines (MOL)[1]. This model was developed to correlate time-dependent relaxation measurements of steady-state CH_4/O_2 flames perturbed by laser photolysis. The conservation of various chemical species mass fractions (Y_k) within the flame is described by a system of coupled nonlinear partial differential equations[2] (PDEs) which depend upon the position, x, relative to the burner surface and the time, t. This system of PDEs and the associated boundary conditions are first discretized in the spatial variable by finite-difference formulae. Thus, the system of PDEs is reduced to a system of coupled ordinary differential equations (ODEs) in time. This system of ODEs is readily integrated using Gears method.[3]

The experiment to be modeled is the 193 nm excimer laser perturbation of a 10 torr CH_4/O_2 flame, Φ = 0.9. The OH and CH concentration profiles as well as the temperature profile throughout the flame have been previously reported for the steady-state flame.[4] In this paper we present the results for OH following perturbation at a position of 3 cm in the post-flame region. As a result of the 193 nm perturbation, the OH concentration increases in the irradiated region. Laser-induced fluorescence is used to monitor OH concentration as it decays back to the steady-state value.

II. MODELING

A. Steady-state flame

We used a one-dimensional flame code[5], referred to as PREMIX, developed at Sandia for modeling premixed, laminar flames. The code predicts steady-state species spatial profiles from a given set of input variables which include: a chemical mechanism, total pressure, inlet gas composition, mass flux, and a vertical temperature profile. PREMIX uses CHEMKIN-II[6] and the Sandia thermodynamic data base[7] to calculate both forward and reverse chemical reaction rates as functions

of pressure, composition and temperature. The mass fluxes due to diffusion are computed from effective binary diffusivities[8] for the gas mixture utilizing Sandia's Transport Code[9] and the Lennard-Jones parameters for the various chemical species in the mechanism. Thermal diffusion (Soret effect) is neglected in the present calculations. The boundary conditions are that the mass flux fraction of each specie be specified at the origin and the spatial derivatives of each mass fraction go to zero downstream of the flame region. We chose the chemical mechanism of Miller and Bowman,[10] deleting reactions involving nitrogen. The resulting chemical mechanism consists of 33 chemical species and 150 chemical reactions along with their rate parameters.

The equation governing the spatial distribution of the k^{th} species in a constant pressure, one-dimensional, laminar flame is

$$\rho(\partial Y_k/\partial t) = \dot{\omega}_k W_k - \rho u(\partial Y_k/\partial x) - \partial(\rho Y_k V_k)/\partial x \ , \qquad (1)$$

where Y_k denotes the mass fraction of the k^{th} species (k=1,33), x the spatial coordinate, t the time, ρ the mass density, W_k the molecular weight of the k^{th} species, $\dot{\omega}_k$ the molar production rate by chemical reaction of the k^{th} species per unit volume and V_k the diffusion velocity of the k^{th} species defined by

$$V_k = v_k - u, \qquad (2)$$

where v_k denotes the velocity of the k^{th} species with respect to a stationary coordinate frame and u, the mass-averaged velocity, is given by

$$u(x) = \sum_k Y_k(x) v_k(x) . \qquad (3)$$

In a burner-stabilized flame, the mass flux (ρu) is a known constant and the molar production rates, $\dot{\omega}_k$, are dependent on the temperature, pressure and composition. These rates are calculated from CHEMKIN-II. The Sandia code solves the steady-state version of Eqn. (1) via a damped Newton method. If convergence difficulties are encountered, a time integration procedure, based upon an Euler algorithm, is implemented to provide a better estimate of the solution. Computations have been carried out on a VAX 6310 computer, where typical computational (CPU) time is less than 30 minutes.

B. TDFLM: Time-dependent flame model

The initial conditions following laser photolysis for the system of ODEs depend upon specific assumptions about the flame and the perturbation laser wavelength. In the post-flame region of our 10 torr CH_4/O_2 flame only H_2O and O_2 have any appreciable absorption at 193 nm. We observe a prompt formation of OH ground-state radicals which relax back to the steady-state with a lifetime of 5 μs. The increased OH, H, and O concentrations and the decreased H_2O and O_2 concentrations from their steady-state values can then be used as the initial conditions for the time-dependent calculation. In the present paper we consider only water photolysis in calculating the initial conditions.

The steady-state flame solutions generated from PREMIX represent the relaxed state of the perturbation experiments. The relaxation after the perturbation is measured in real time and one must have an accurate time-integration scheme to model the experiments. In the MOL algorithm the spatial derivatives on the right-hand side of Eqn. (1) are replaced by finite-difference expressions, reducing the PDEs to a system of ODEs for $Y_k(j,t)$. Each j corresponds to a specified spatial

position above the burner surface. Thus, Eqn. (1) becomes

$$dY_k/dt = \text{Chemistry} - \text{Convection} - \text{Diffusion}, \qquad (4)$$

where

$$\text{Chemistry} = \dot{\omega}_k W_k/\rho$$

$$\text{Convection} = u_j[Y_k(j,t) - Y_k(j-1,t)]/[x_j - x_{j-1}]$$

$$\text{Diffusion} = [(\rho Y_k V_k)_{j+1/2} - (\rho Y_k V_k)_{j-1/2}]/[x_{j+1/2} - x_{j-1/2}]$$

Pictorially, this method divides the one-dimensional flame into a number of spatial slices, as represented in Figure 1. The center of each slice corresponds to a particular height above the burner surface. The temporal evolution of the chemical species is computed within each slice along a line parallel to the time axis. This computation is done by Gear's method using DGEAR,[3] an IMSL (International Math Science Library) subroutine. The complete solution of these equations requires appropriate boundary conditions and initial conditions. TDFLM computes a starting set of mole fractions at time zero by first reading the steady-state results from the PREMIX calculation for the corresponding position in the flame. The code includes a photolysis mechanism which can alter the concentration of one or more species. The boundary conditions are chosen to correspond to the steady-state PREMIX calculation, i.e., mole fractions are specified upstream (at the burner surface), and spatial derivatives vanish downstream (at the end of the post flame region).

III. DISCUSSION

In the experiment we perturbed a position in the flame 3 cm above the burner surface, which has a measured OH rotational temperature of 1770 $\pm$ 60 K, using an ArF excimer laser. The laser beam was masked to produce a measured width of 3 mm and an intensity of 4.0 $\pm$ 3.2 J/cm^2. There is a 117 $\pm$ 15% observed maximum OH concentration increase over the steady-state as a result of the perturbation. This corresponds to photolysis of 7.5% of the water at this height above the burner (based on the PREMIX results). Using temperature dependent absorption coefficients for H_2O and O_2,[11] and an observed increase in OH of 117% over the steady-state, the excimer laser intensity is estimated to be 1.2 J/cm^2. This estimate is consistent with the experimental number. Photolysis of 7.5% of the steady-state water concentration to produce OH and H is utilized as input to the TDFLM code. Concentrations for the perturbed condition are converted to renormalized mass fractions for all chemical species by the TDFLM code. The TDFLM code then calculates the relaxation of the OH concentration back to the steady-state solution. Figure 2 shows the experimental OH decay following the 193 nm laser perturbation (open circles). The experimental steady-state solution is indicated by the filled square, with $\pm$ 2σ experimental uncertainty. As can be seen in Figure 2, the OH concentration returns to its steady-state within 15 μs. The filled circles in Figure 2 are a least-squares fit of the experimental data to a single exponential. Error bars on the least-squares fit are a $\pm$ 1σ confidence limit. Figure 3 shows the results of the TDFLM calculation. The axis on the left is the same as Figure 2. The right axis in Figure 3 corresponds to the calculated OH concentration. The filled circles in this figure are taken from Figure 2. The dashed line in Figure 3 results from dropping the diffusion and convection terms in Eqn. (4).

This calculation predicts the OH concentration to decay to a value which is larger than the PREMIX steady-state value. Separate numerical calculations demonstrate that chemistry dominates the short time relaxation. However, in the long time limit the purely kinetic calculation predicts an equilibrium concentration which is slightly greater than the experimentally observed value.

The solid line in Figure 3 is calculated from Eqn. (4) where terms for diffusion, convection and chemistry are included in the calculation. The agreement between the calculated behavior and the experimental observation is good. The binary diffusion coefficient for most gases at 1 atm pressure is on the order of 0.1 cm^2/s.[12] The diffusion coefficient increases with temperature ($T^{3/2}$ dependence) and is inversely proportional to pressure.[13] At 1770 K and 10 torr, diffusion coefficients are on the order of 1000 cm^2/s. Neglecting the diffusion and convection terms in the calculation is equivalent to assuming a homogeneous gas-phase reaction at 1770 K in a closed system. The relative OH concentration decreases more rapidly when mass transport effects are included in Eqn. (4). In the long time limit these terms contribute to a steady-state balance which lies within the error bars of the experiment. At this position in the post-flame, the OH concentration gradient is relatively small, and the net effects of the transport terms is less than 10%.

Future studies will examine the effect of including the photolysis of O_2 in the perturbation mechanism. Also, calculations to model perturbation in the flame zone are planned. In the flame zone, large concentration gradients make the transport terms more important and essential for modeling the observed relaxation.

IV. ACKNOWLEDGEMENTS

We would like to thank Robert Kee and Sandia National Laboratories for providing the Sandia codes.

V. REFERENCES

1. Galant, S., Eighteenth Symposium (International) on Combustion, (The Combustion Institute, 1981) pp 1451-1459.
2. Kuo, K.K., Principles of Combustion, (John Wiley & Sons, New York, 1986) ch. 3.
3. Gear, C.W., "The Automatic Integration of Ordinary Differential Equations", Comm. A.C.M., **14**, pp 176-179 (1971). See also IMSL, User's Manual, Vol. 1, Edition 9.2, IMSL Inc., 7500 Bellaire Boulevard, Houston, TX, U.S.A. (1984).
4. Fleming, J.W., Burton, K.A., and Ladouceur, H.D., "OH and CH profiles in a 10 Torr methane/oxygen flame: experiment and flame modeling," Chem. Phys. Lett. **175** (4), 395-400 (1990).
5. R.J. Kee, J.F. Grcar, M.D. Smooke, and J.A. Miller, "A Fortran Program for Modeling Steady Laminar One-Dimensional Premixed Flames," Sandia Report SAND85-8240 (1987).
6. R.J. Kee, F.M. Rupley, and J.A. Miller,"Chemkin-II: A Fortran Chemical Kinetics Package for the Analysis of Gas-Phase Chemical Kinetics," Sandia Report SAND 89-8009 (1989).
7. R.J.Kee, F.M. Rupley, and J.A. Miller,"The CHEMKIN Thermodynamic Data Base," Sandia Report SAND87-8215 (1989).
8. Curtis, C.F. and Hirshfelder, J.O., "Transport Properties of Multicomponent Gas Mixtures," J. Chem. Phys., **17**, p 550-555 (1949).
9. R.J. Kee, J. Warnatz, and J.A. Miller,"A FORTRAN Computer Code

Package for the Evaluation of Gas-Phase Viscosities, Conductivities, and Diffusion Coefficients," Sandia Report SAND 83-8209 (1983).
10. Miller, J.A. and Bowman, C.T., "Mechanism and Modeling of Nitrogen Chemistry in Combustion," Prog. Energy Combust. Sci. 15, pp 287-338 (1989).
11. Davidson, D.F., Chang, A.Y., Kohse-Höinghaus, K., and Hanson, R.K., "High Temperature Absorption Coefficients of O_2, NH_3, and H_2O for Broadband ArF Excimer Laser Radiation," J. Quant. Spectrosc. Radiat. Transfer, 42, No. 4, pp 267-278 (1989).
12. Bird, R.B., Stewart, W.E., and Lightfoot, E.N., Transport Phenomena, (John Wiley and Sons, New York, 1960) p 503.
13. ibid p 510.

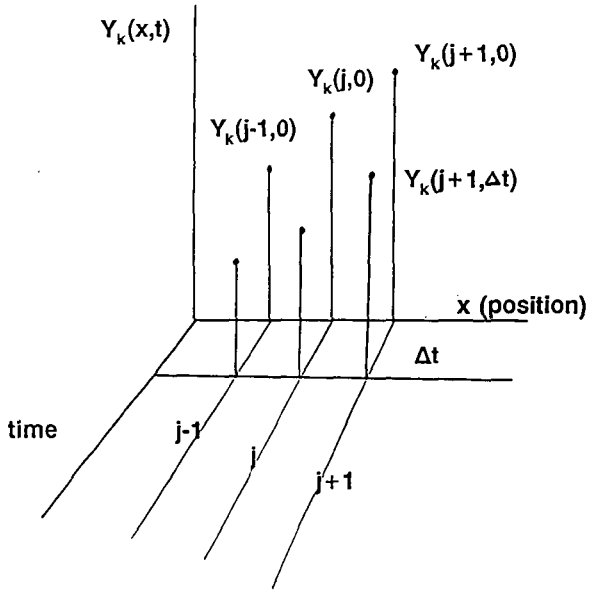

Figure 1. Schematic for the method of lines algorithm. Y_k denotes the k^{th} species mass fraction at position j above the burner at time t.

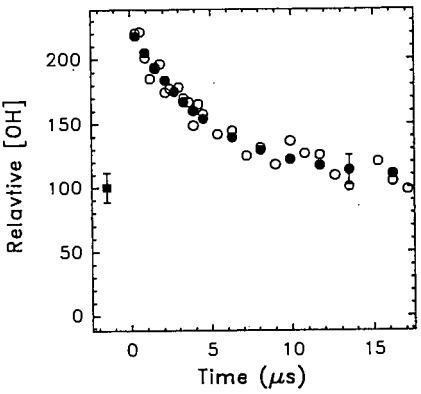

Figure 2. Relative experimental OH concentration at 3 cm above the burner surface in a 10 torr CH_4/O_2 flame as a function of time following 193 nm perturbation (open circles); Least-squares fit of the experimental OH decay to a single exponential (filled circles); relative experimental OH steady-state concentration (filled square). Error bars on the least-squares fit are a $\pm$ 1σ confidence limit.

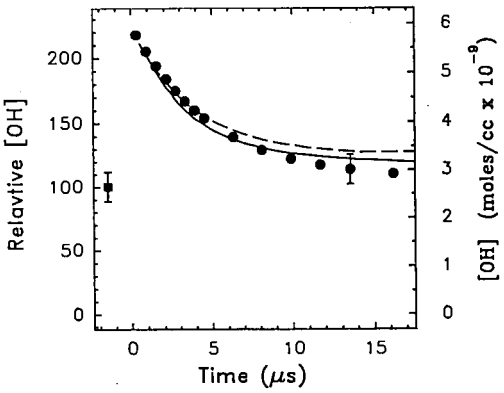

Figure 3. Least-squares fit of the relative experimental OH concentration at 3 cm above the burner surface in a 10 torr CH_4/O_2 flame as a function of time following 193 nm perturbation (filled circles, left axis); relative experimental OH steady-state concentration (filled square,left axis); TDFLM calculation with transport and chemistry (solid line, right axis); TDFLM calculation with no transport terms (dashed line, right axis). Error bars on the experimental steady-state represent $\pm$ 2σ experimental uncertainty. Error bars on the least-squares fit are a $\pm$ 1σ confidence limit. The left and right vertical axes have been chosen so that the relative experimental steady-state concentration equals the calculated PREMIX value.